Electronic Supplementary Material (ESI) for Energy & Environmental Science.
This journal is © The Royal Society of Chemistry 2021

Supporting Information

Grafted MXene/Polymer Electrolyte for High Performance Solid Zinc Batteries with Enhanced Shelf Life at Low/High Temperatures

Ze Chen,[1#] Xinliang Li,[1#] Donghong Wang,[1] Qi Yang,[1] Longtao Ma,[1] Zhaodong Huang,[1] Guojing Liang,[1] Ao Chen,[1] Ying Guo,[1] Binbin Dong,[4] Xingyi Huang,[5] Cheng Yang,[6] Chunyi Zhi*[1,2,3]

[1]Department of Materials Science and Engineering, City University of Hong Kong, 83 Tat Chee Avenue, Kowloon, Hong Kong 999077, China.

[2]Centre for Functional Photonics, City University of Hong Kong, Kowloon, Hong Kong.

[3]Center for Advanced Nuclear Safety and Sustainable Development, City University of Hong Kong, Kowloon, Hong Kong.

[4]National Engineering Research Center for Advanced Polymer Processing Technology, Zhengzhou University, Zhengzhou, Henan 450002, China.

[5]Shanghai Key Laboratory of Electrical Insulation and Thermal Ageing, State Key Laboratory of Metal Matrix Composites, Shanghai Jiao Tong University, Shanghai 200240 China.

[6]Institute of Materials Research, Tsinghua Shenzhen International Graduate School, Tsinghua Campus, Shenzhen, Guangdong 518055, China.

mail: cy.zhi@cityu.edu.hk

[#]The two authors contribute equally to this work.

Experimental Section

Materials: poly(vinylidene fluoride-co-hexafluoropropylene) (PVHF, average Mn ~130,000,) is purchased from Sigma Aldrich. Ti_3AlC_2 ceramics powder is directly purchased from 11 Technology Co., Ltd. Methyl acrylate (MA), N, N-Dimethylformamide (DMF), magnesium sulfate ($MnSO_4$) and potassium ferricyanide ($K_3Fe(CN)_6$) zinc trifluoromethanesulfonate ($Zn(OTF)_2$) and ceric ammonium nitrate (CAN) are purchased from Aladdin. The purchased methyl acrylate needs to undergo vacuum distillation to remove the inhibitor.

Preparation of MXene layers: To selectively etch Al from Ti_3AlC_2, 1 g of Ti_3AlC_2 ceramics powder with mesh size≤45 μm was slowly added to 20 mL of etchant containing a mixture of 15 ml HCl and 5 ml deionized water. The solution was stirred in water bath under 40 ^oC for 48 h. The single layered $Ti_3C_2T_x$ MXene was washed repeatedly with deionized water by centrifugation at 3500 rpm and the product was collected.

Preparation of poly (methyl acrylate) grafted MXene (MXene-g-PMA): First, the MXene solution containing 50 mg MXene solid was dispersed in water to 100 ml and sonicated in sonic bath for 30 min followed by introducing 20 mL of CAN in 1 mol/L nitric acid solution. Then, under nitrogen atmosphere, the MA monomer was added to the solutions by drops. The polymerization experiment was carried out at 70 ^oC for 6 h. After polymerization, the products were collected by vacuum filtration, washed by alcohol and DMF to get rid of the residual monomers and free polymers. The brown product was re-dispersed into DMF via stirring for 12 h. Finally, a black solution was obtained.

Preparation of solid polymer electrolytes (SPEs): PVHF and $Zn(OTF)_2$ with a weight ratio of 10 : 1 were dissolved in DMF. Colloidal PMA-grafted MXene suspension was then added to the

mixture. The flask was sealed, and the suspension was stirred at 40 °C for 6 h, sonicated for 10 min and then casted onto a glass plate to evaporate the solvent at room temperature. Membranes were obtained after further drying at 70 °C under vacuum for five days, and then at 120 °C for 4 h under vacuum. Three different contents of MXene-g-PMA were introduced into the system, denoted as PVHF/MXene-g-PMA^{x}, where the superscript x is the weight ratio of MXene-g-PMA to PVHF, controlled to be 0.01, 0.05, and 0.1. In addition, to verify the effect of polymer grafting in the system, undecorated MXene was also added into the PVHF/$Zn(OTF)_2$ matrix to form the control sample PVHF/MXene. All membranes were stored in a glove box (H_2O < 1 ppm, O_2 < 1 ppm) for at least one week before being tested.

Preparation of manganese hexacyanoferrate (MnHCF): MnHCF nanoparticles were synthesized by a standard coprecipitation method.[1] Typically, 100 ml of $MnSO_4$ (0.06 M) aqueous solution was added dropwise under stirring, into 100 ml of $K_3Fe(CN)_6$ (0.03 M) solution. The resulting solution was kept stirring at 60 °C for 30 min. After standing for another 3 hours, the precipitates were separated via centrifugation and washed extensively with deionized water and ethanol several times. Brown solids were obtained after dried under vacuum at 60 °C. To prepare the cathode, firstly mixing MnHCF, acetylene blacks and PVDF binder (7:2:1) together in NMP to form a homogeneous slurry, which was then casted onto a piece of carbon cloth followed by drying at 50 °C. The effective mass loading of MnHCF is about 2.1 mg cm^{-2}.

Characterization methods: Transmission electron microscope (TEM) was performed on a JEOL-2001F operated at 200 kV. A field-emission scanning electron microscope (SEM, FEI Quanta 450 FEG) and atomic force microscopy (AFM, Bruker Innova) was used to investigate the morphologies of the products. Thermogravimetric Analysis (TGA) was applied on TG/DTA 6300 to obtain the

polymer content in the composite. Phase composition transition was confirmed by X-ray diffraction equipment (XRD, Bruker D2 Phaser) with Cu Ka radiation at 30 kV. Fourier-transform infrared spectroscopy (FT-IR, PerkinElmer Spectrum II) was used to verify the polymer component. Differential scanning calorimetry (DSC) experiments were conducted using a DSC Q2000 (TA Instruments) with Tzero pans.

Electrochemical measurements: The ionic conductivity was measured based on the stainless steel (SS)/SS coin cell. The SPEs membrane were sandwiched between the two stainless steel blocking electrodes in the cell and following by hot-pressing the cell at 110 ^{o}C for 2 h. Temperature scan of the ionic conductivity of the SPEs with 10 ^{o}C increments was conducted using an oven. A 20 mV ac perturbation and a frequency range of 1 MHz to 0.1 Hz were used for each measurement. The ionic conductivity (s) was calculated assuming:

$$\sigma = L/(A*R)$$

where L and A are the thickness and surface area of the membrane, respectively.

The Zn ion transference numbers, $t_{Zn^{2+}}$, of all the SPEs were measured at 55 ^{o}C. The impedance of the Zn/Zn symmetric cell was measured before and after polarization with a DC voltage pulse (10 mV) with a Gamry Interface 1000 Potentiostat. $t_{Zn^{2+}}$ was calculated assuming:

$$t_{zn^{2+}} = \frac{I_{ss}}{I_0} \times \frac{\Delta V - I_0 R_0}{\Delta V - I_{ss} R_{ss}}$$

where I_{ss} and I_0 are the steady state and initial currents, respectively, and R_{ss} and R_0 are the corresponding steady state and initial resistances.

Linear sweep voltammetry (LSV) measurements were performed at room temperature using a CHI 760D. Zn metal and SS were used as the reference and the working electrodes, respectively. A linear sweep was conducted from 0 V to 3.5 V at a scan rate of 0.1 mV s^{-1}.

Both coin-2032 and pouch cell were assembled for electrochemical measurements. The coin cell used a zinc foil with 0.2 mm thickness as the anode electrode, MnHCF on carbon clothes with 2.1 mg cm^{-2} loading mass as the cathode with the as-prepared SPEs. For pouch cell, zinc foil with 0.1 mm thickness was used as the anode. The cyclic performance, electrochemical properties of batteries were characterized by the LAND CT2001A device and electrochemical workstation CHI 760D at various temperature.

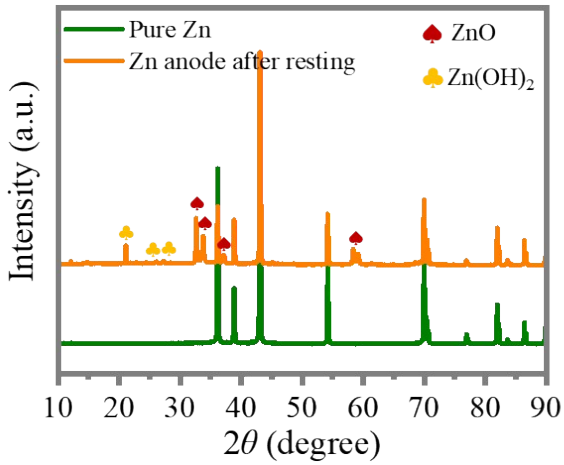

Figure S1. XRD patterns of pure Zn and Zn anode from Zn/MnHCF pouch cell rested for two weeks. The morphology change of Zn anode after resting are attributed to formation of ZnO and $Zn(OH)_2$.

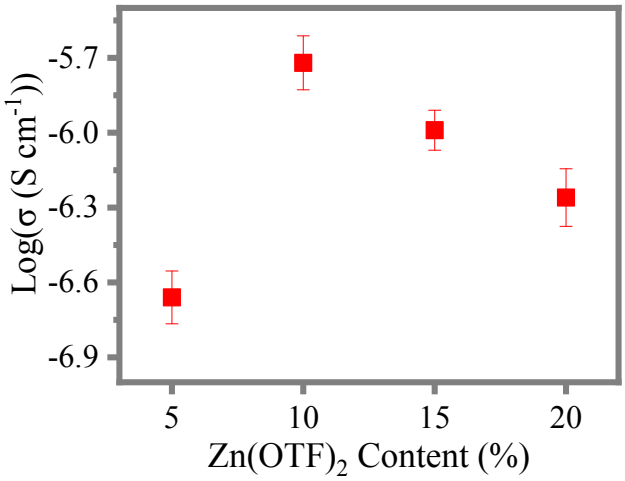

Figure S2. Ionic conductivity of PVHF based SPEs with different content of $Zn(OTF)_2$.

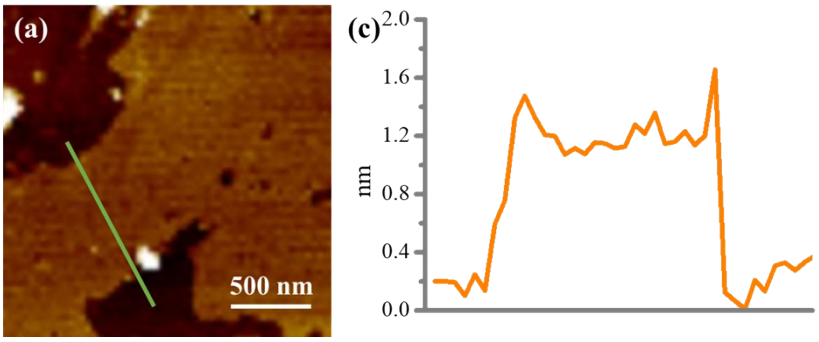

Figure S3. MXene nanosheets: a) AFM image and b) the height profile.

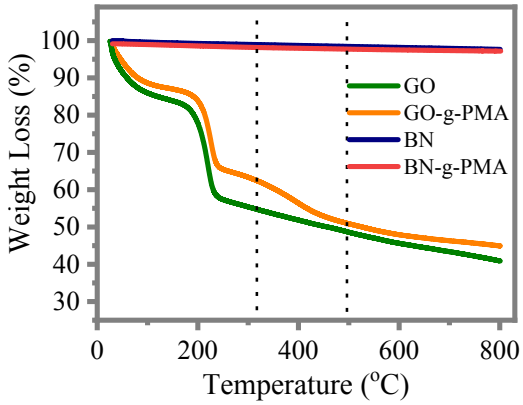

Figure S4. TGA curves of BN, BN-g-PMA, GO and GO-g-PMA.

After the same preparation procedures of MXene-g-PMA, the grafting density of BN-g-PMA and GO-g-PMA can be calculated as 0.85% and 11.2%, respectively.

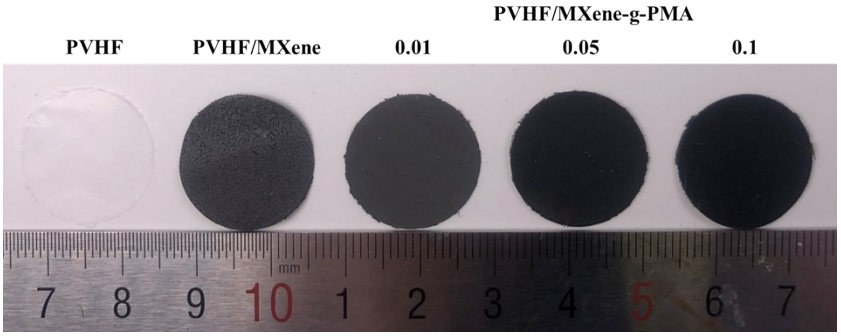

Figure S5. Pictures of SPEs: PVHF, PVHF/MXene, PVHF/MXene-g-PMA$^{0.01}$, PVHF/MXene-g-PMA$^{0.05}$ and PVHF/MXene-g-PMA$^{0.1}$.

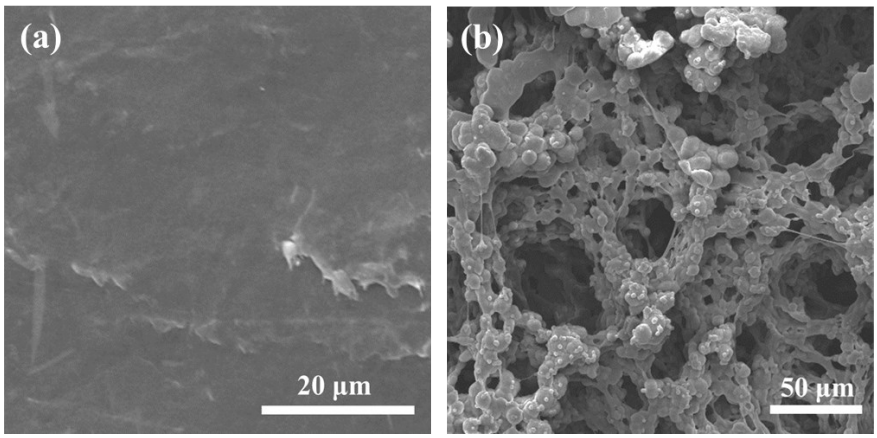

Figure S6. SEM images of SPEs: a) PVHF; b) PVHF/MXene.

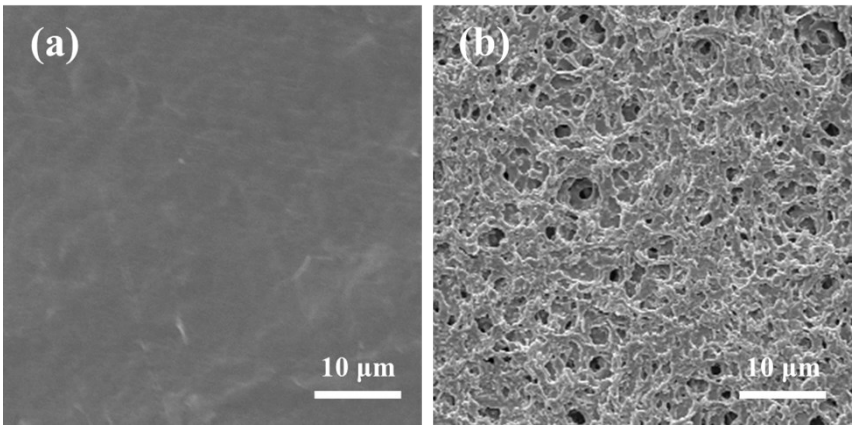

Figure S7. SEM images of SPEs: a) PVHF/MXene-g-PMA$^{0.01}$; b) PVHF/MXene-g-PMA$^{0.1}$.

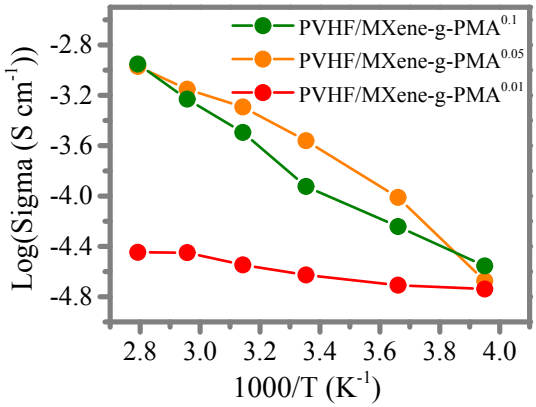

Figure S8. Temperature scan of the ionic conductivities of PVHF/MXene-g-PMA^{x} (x=0.01, 0.05 and 0.1).

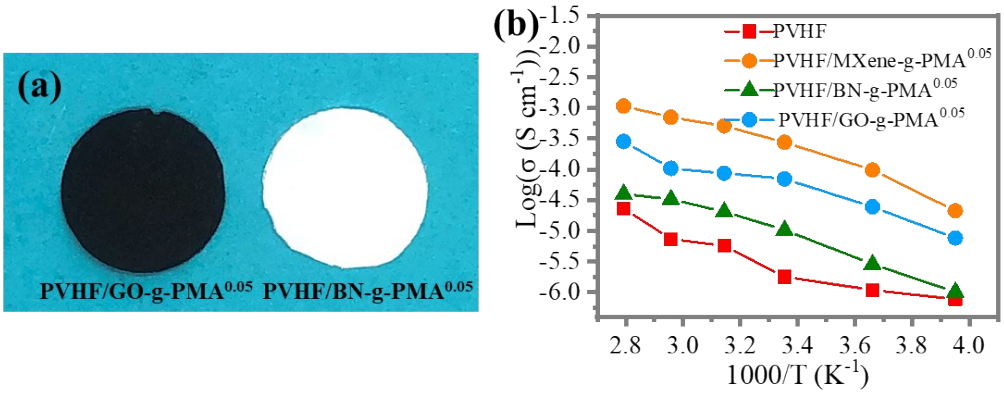

Figure S9. a) pictures of PVHF/GO-g-PMA$^{0.05}$ and PVHF/BN-g-PMA$^{0.05}$; b) ionic conductivity of PVHF/GO-g-PMA$^{0.05}$ and PVHF/BN-g-PMA$^{0.05}$.

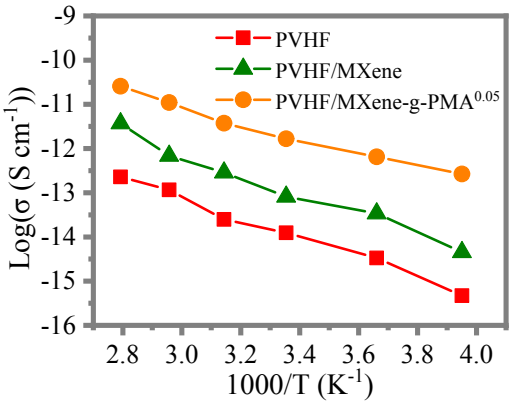

Figure S10. Electrical conductivity of the as-prepared SPEs at different temperatures.

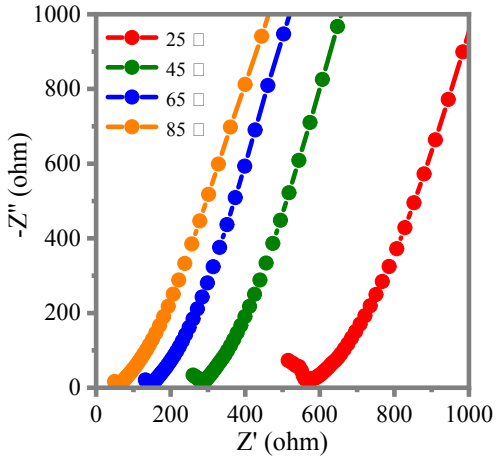

Figure S11. EIS curves of PVHF/MXene-g-PMA$^{0.05}$ at different temperatures.

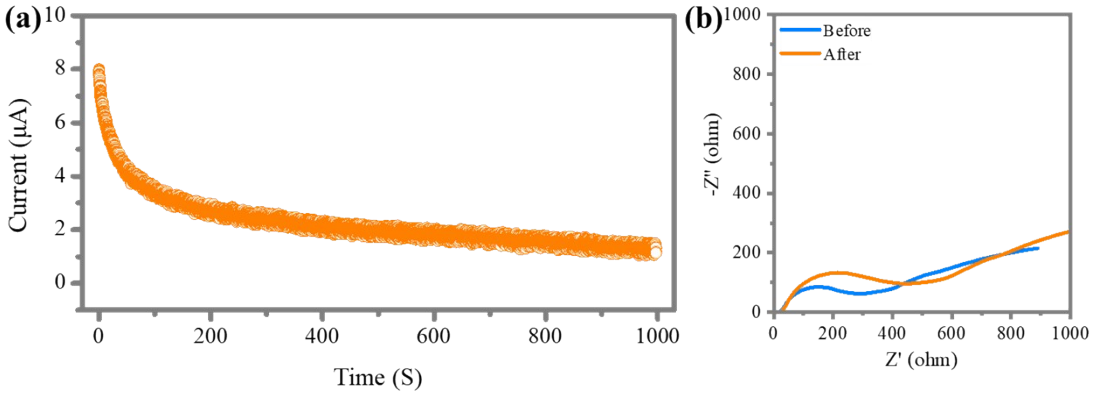

Figure S12. Zn^{2+} transference number measurement of the PVHF/MXene-g-PMA$^{0.05}$. a) the symmetric Zn/PVHF/MXene-g-PMA$^{0.05}$/Zn cell at the direct current bias of 20 mV; b) corresponding impedance measurements performed at the initial state and steady-state.

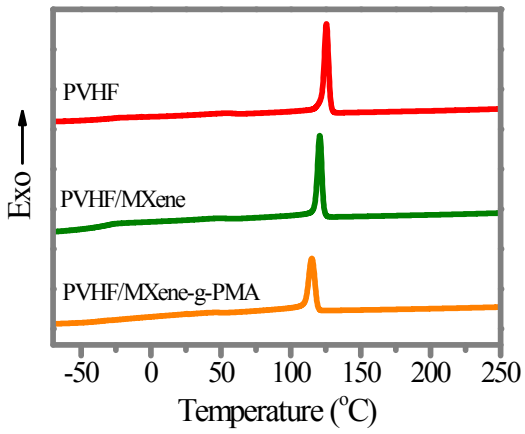

Figure S13. DSC thermograms obtained at a rate of 10 °C min^{-1} during first cooling.

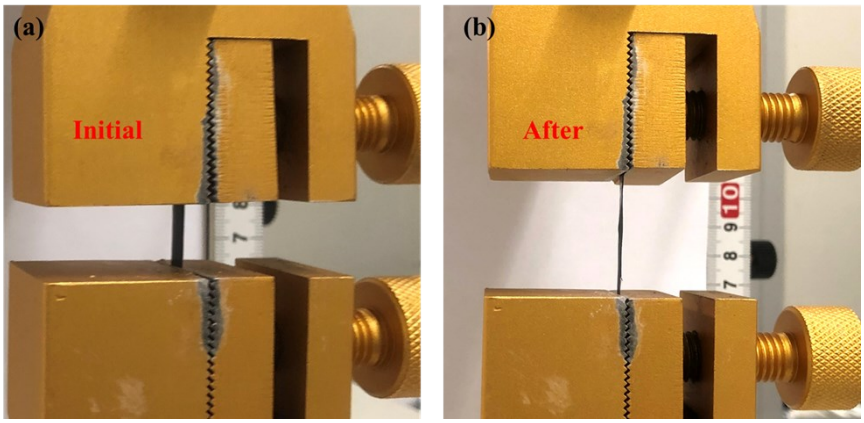

Figure S14. Pictures of PVHF/MXene-g-PMA$^{0.05}$ SPEs under the tensile test.

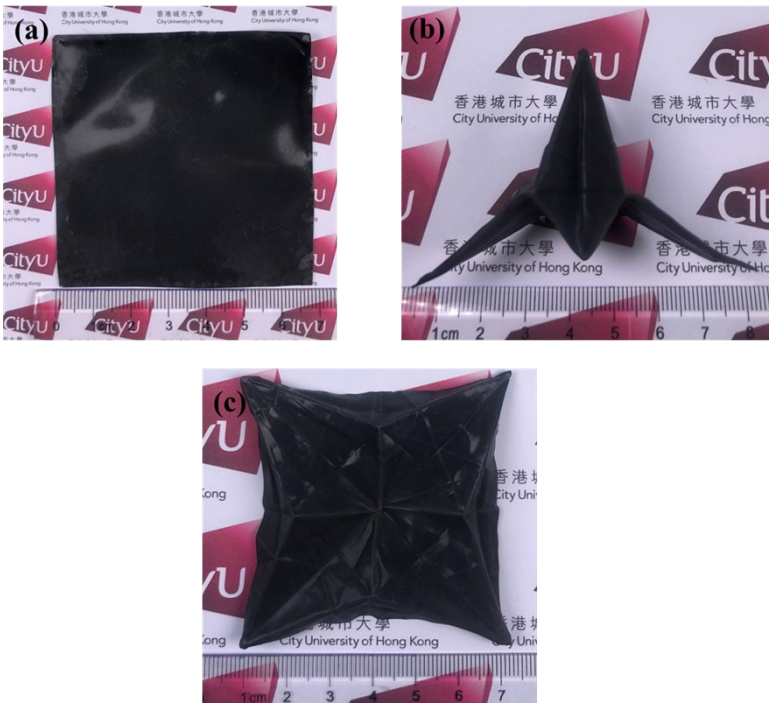

Figure S15. Pictures of PVHF/MXene-g-PMA$^{0.05}$ membrane after folding and opening.

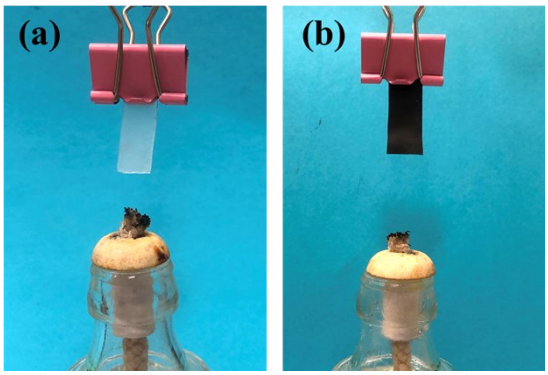

Figure S16. Pictures of flame test on the PVHF SPEs and the PVHF/MXene-g-PMA$^{0.05}$ SPEs.

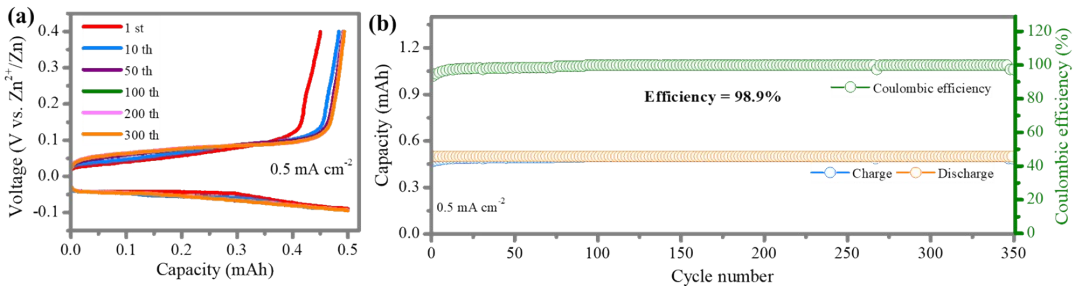

Figure S17. a) voltage profile of a Zn/Cu cell in PVHF/MXene-g-PMA$^{0.05}$ SPEs at a current density of 0.5 mA cm^{-2}. b) corresponding cyclic performance test.

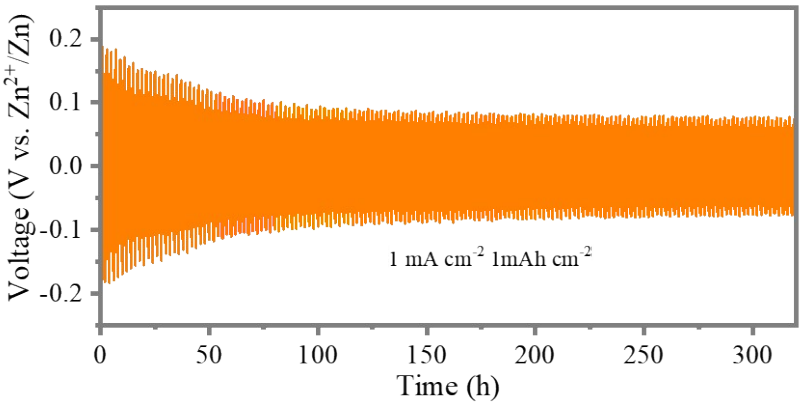

Figure S18. Galvanostatic Zn plating/stripping in Zn/Zn symmetrical cells with a current density of 1 mA cm^{-2} and a capacity of 1 mAh cm^{-2}.

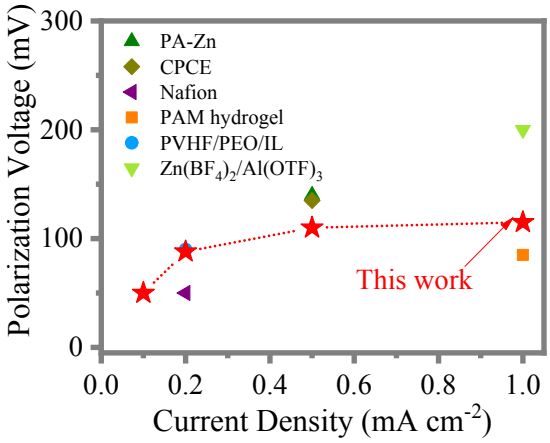

Figure S19. Comparison of polarization potentials of Zn//Zn symmetrical cells at different current densities with other reports.[2-7]

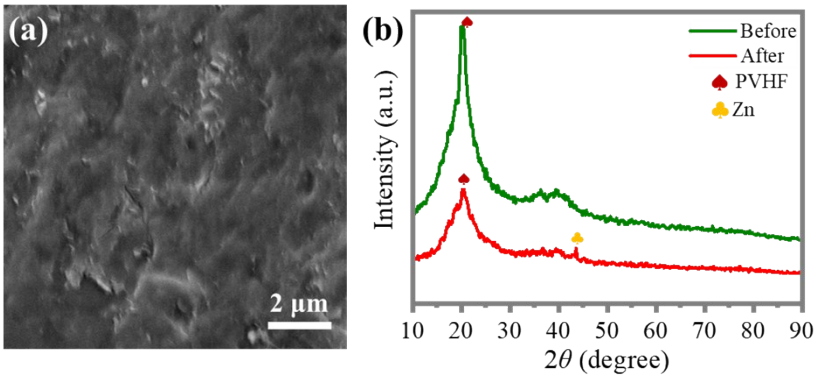

Figure S20. a) SEM picture of the PVHF/MXene-g-PMA$^{0.05}$ after cycling and b) the XRD patterns of PVHF/MXene-g-PMA$^{0.05}$ before and after cycling.

After cycling, the surface morphology and the phase structure of the PVHF/MXene-g-PMA$^{0.05}$ SPE almost remains unchanged, demonstrating the high stability of SPE and the homogeneous Zn deposition during cycling. In addition, a new peak was generated in the XRD pattern of the SPE after cycling, originating from the residual zinc deposit when the zinc sheet was detached from the SPE.

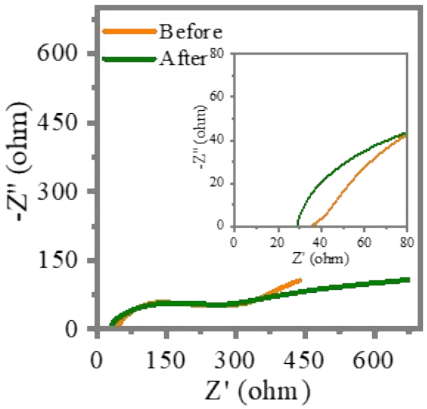

Figure S21. EIS curves of Zn//Zn symmetrical cell before and after cycling.

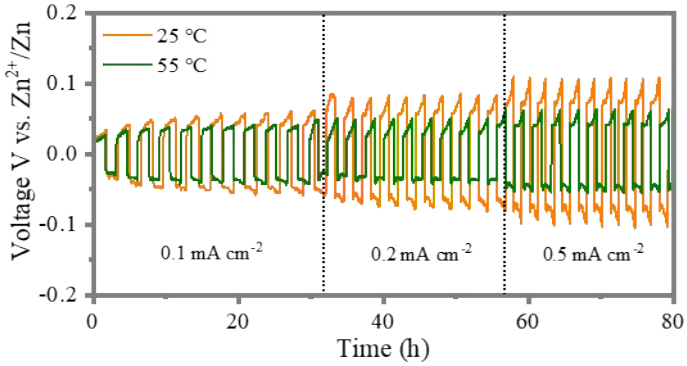

Figure S22. Galvanostatic Zn plating/stripping in Zn/Zn symmetrical cells based on the PVHF/MXene-g-PMA$^{0.05}$ at 25 °C and 55 °C.

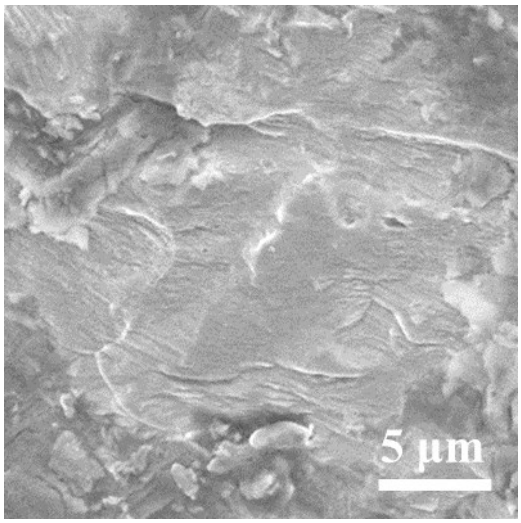

Figure S23. SEM images of Zn anode after 200 h plating/striping at 0.5 mA cm^{-2} and 0.5 mAh cm^{-2} at 55 °C.

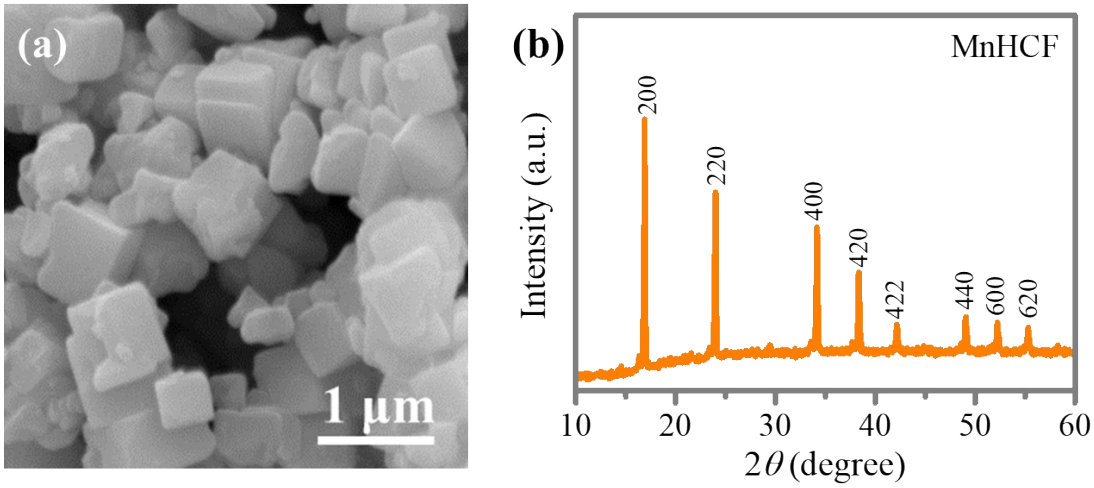

Figure S24. a) SEM image of MnHCF; b) XRD pattern of MnHCF.

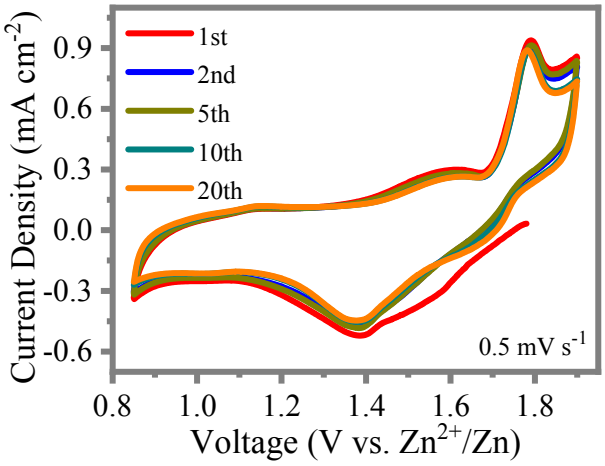

Figure S25. CV curves of Zn/MnHCF full cell at the scan rate of 0.5 mV s^{-1}.

References

1. D. Wang, H. Lv, T. Hussain, Q. Yang, G. Liang, Y. Zhao, L. Ma, Q. Li, H. Li, B. Dong, T. Kaewmaraya and C. Zhi, *Nano Energy*, 2021, **84**, 105945.
2. L. Ma, S. Chen, N. Li, Z. Liu, Z. Tang, J. A. Zapien, S. Chen, J. Fan and C. Zhi, *Advanced Materials*, 2020, **32**, 1908121.
3. D. Yuan, W. Manalastas Jr., L. Zhang, J. J. Chan, S. Meng, Y. Chen and M. Srinivasan, 2019, **12**, 4889-4900.
4. Q. Zhang, J. Luan, L. Fu, S. Wu, Y. Tang, X. Ji and H. Wang, 2019, **58**, 15841-15847.
5. Z. Zhao, J. Zhao, Z. Hu, J. Li, J. Li, Y. Zhang, C. Wang and G. Cui, *Energy & Environmental Science*, 2019, **12**, 1938-1949.
6. L. Ma, S. Chen, X. Li, A. Chen, B. Dong and C. J. A. C. Zhi, 2020, **132**, 24044-24052.
7. F. Mo, Z. Chen, G. Liang, D. Wang, Y. Zhao, H. Li, B. Dong and C. Zhi, *Advanced Energy Materials*, 2020, **10**, 2000035.